Nano Research 2017, 10(6): 2146–2155
DOI 10.1007/s12274-016-1404-3
Research Article
ISSN 1998-0124
CN 11-5974/O4

Cooperative interactions among CTA^+, Br^- and Ag^+ during seeded growth of gold nanorods

Yong Xu[1], Lei Chen[1], Xingchen Ye[2], Xuchun Wang[1], Jiaqi Yu[1], Yang Zhao[1], Muhan Cao[1], Zhouhui Xia[1], Baoquan Sun[1] (✉), and Qiao Zhang[1] (✉)

[1] *Jiangsu Key Laboratory for Carbon-Based Functional Materials & Devices, Institute of Functional Nano and Soft Materials (FUNSOM), Soochow University, Suzhou 215123, China*
[2] *Department of Chemistry, University of California Berkeley, Berkeley, CA 94720, USA*

Received: 21 July 2016
Revised: 28 November 2016
Accepted: 3 December 2016

KEYWORDS
gold nanorods, anisotropic nanostructure, surface plasmon resonance, seeded growth, cetyltrimethyl ammonium bromide (CTAB)

ABSTRACT

We have carried out a comprehensive study on the formation mechanism of Au nanorods (AuNRs) in binary surfactant mixtures composed of quaternary ammonium halide and sodium oleate (NaOL). We identify the cetyltrimethyl ammonium (CTA)-Br-Ag^+ complex as the key ingredient in directing the anisotropic growth of AuNRs. Based on the improved understanding of the cooperative interactions among CTA^+, Br^- and Ag^+, we further demonstrate that AgBr, which is readily solubilized by the cetyltrimethyl ammonium bromide (CTAB) or cetyltrimethyl ammonium chloride (CTAC) micelles, can be employed as the combined source of Ag^+ and Br^- for the preparation of AuNRs. The growth of high-quality AuNRs can be completed within 15 min under extremely low bromide content (0.1 mM).

1 Introduction

Anisotropic nanostructures have drawn great attention from the research community due to their size- and shape-dependent physical properties [1–5]. Among these nanostructures, colloidal gold nanorods (AuNRs) have become one of the most widely studied model nanostructures over the past decade because of their unique surface plasmon resonance (SPR) property [6] and their potential applications in biomedical imaging [7–14], therapy [15–19], and surface-enhanced Raman scattering (SERS) [20–24]. The first reported synthesis of "true" AuNRs dates back to the mid-1990s, when Wang and co-workers prepared AuNRs with distinctive SPR using an electrochemical approach [25]. A significant boost in AuNRs research has been spurred by the pioneering work on silver-assisted seed-mediated synthesis of AuNRs from the Murphy group and the El-Sayed group in the early 2000s [26–28]. Since then, continuous effort has been devoted to optimizing the

Address correspondence to Qiao Zhang, qiaozhang@suda.edu.cn; Baoquan Sun, bqsun@suda.edu.cn

original protocol and impressive progress has been made. For example, various types of additives, including nitric acid or hydrochloric acid [29–31], sulfides [32], halides (bromide and iodide) [33–36], and acetone [26], have been used to initiate and control the growth of AuNRs. Recently, by introducing aromatic additives or secondary surfactants as a weak reducing agent, Murray and co-workers were able to synthesize monodisperse AuNRs with broadly tunable aspect ratio and SPR peaks [37–39]. Although significant progress has been made on the mechanistic understanding of AuNRs through the use of various *ex situ* and *in situ* characterization techniques, many key components of the growth system remain poorly understood. Since the synthesis involves multiple reagents and reaction steps, it has been very difficult to directly probe the roles of individual ingredients of the reaction mixture.

It is generally accepted that Au seeds, CTA^+, Br^- and Ag^+, are collectively responsible for the formation of AuNRs. Gold seeds (about 3 nm) with different crystallinities can lead to the formation of either penta-twinned or single-crystal AuNRs [40]. The CTA^+ ions were originally considered as a soft-template to direct the growth of AuNRs, but later it became widely accepted that CTA^+ ions form a bi-layer around the AuNRs and act as a capping ligand. In contrast, the role of Br^- has been a subject of debate. Both the Murphy and Jin groups reported that a high concentration of Br^- (0.1 M) was needed to obtain high-quality AuNRs [36, 41]. Jin and co-workers also proposed that a high concentration of Br^- could etch the Au seeds and facilitate the formation of AuNRs [41].

However, Murray and co-workers reported that monodisperse AuNRs can still be obtained at a low concentration of Br^- (~0.15 mM) [37]. Furthermore, Ag^+ is important for improving the product yield and controlling the aspect ratio of AuNRs.

There are three major hypotheses for the role of Ag^+: (1) under-potential deposition (UPD) of silver on AuNRs: A sub-monolayer of Ag atoms could be deposited onto the side facet of AuNRs and therefore ensure the anisotropic growth [42, 43]; (2) facet-blocking: The CTA-Br-Ag-Br complex can selectively adsorb onto the side facet of AuNRs and block the growth perpendicular to that direction [44–46]; (3) soft-templating: Ag^+ can interact with Br^- and deform the shape of CTAB micelles from spherical to cylindrical [40, 47].

However, none of these hypotheses can satisfactorily account for all of the experimental observations. For instance, metallic silver has been detected near the surface of AuNRs through X-ray photoelectron spectroscopy (XPS) and extended X-ray absorption fine structure (EXAFS) characterizations, supporting the UPD mechanism. On the other hand, using advanced energy dispersive X-ray spectroscopy, Wright and co-workers showed that there was no preferential adsorption of Ag^+ on certain facets around the surface of AuNRs, in consistent with the "soft-template" mechanism [48].

In this contribution, we study the roles of key reactants in the Ag^+-assisted seed-mediated growth of AuNRs in a binary surfactant system. We identified the function of each component by replacing cetyltrimethyl ammonium bromide (CTAB) with a mixture of cetyltrimethyl ammonium chloride (CTAC) and KBr. It is found that seeds capped with either CTAB or CTAC can lead to the formation of AuNRs in high yields. To ensure high-yield synthesis of AuNRs, there exists a minimally required concentration for the Br^- and Ag^+ (~0.1 mM for both). Importantly, we find that the ratio of Br^-/Ag^+ should be equal to or greater than 1:1 when the concentrations of both species approach the minima (~0.1 mM for both), indicating that there is a synergetic interaction between Ag^+ and Br^- in directing the formation of AuNRs.

2 Experimental

2.1 Chemicals

CTAB (>98.0%), CTAC (or C16, >95.0%), tetradecyltrimethyl ammonium chloride (TTAC) (or C14, >98.0%), dodecyltrimethyl ammonium chloride (DTAC) (or C12, >97.0%), octadecyltrimethyl ammonium chloride (OTAC) (or C18, >98.0%) and sodium oleate (NaOL, >97.0%) were purchased from TCI China. Hydrogen tetrachloroaurate trihydrate ($HAuCl_4 \cdot 3H_2O$), L-ascorbic acid (BioUltra, ≥99.5%), silver nitrate ($AgNO_3$, >99%), sodium borohydride ($NaBH_4$, 99%), and hydrochloric acid (HCl, 37 wt.% in water, 12.1 M) were purchased from Sigma Aldrich. All chemicals were used as received. Ultrapure water obtained from a Milli-Q

Integral 5 system was used for all experiments. All glassware was cleaned with freshly prepared aqua regia (HCl and HNO_3 in a 3:1 volume ratio), followed by rinsing with copious amount of water.

2.2 Synthesis of AuNRs

AuNRs were synthesized according to the following three steps. (1) Preparation of growth solution: Certain amounts of CTAC and sodium oleate were dissolved in water, after which $HAuCl_4$ solution was added. (2) Preparation of seed solution: 5 mL of CTAC solution (0.2 M) was mixed with 5 mL of $HAuCl_4$ (0.5 mM) solution in a 20 mL glass vial. 0.6 mL of fresh $NaBH_4$ (0.01 M) was diluted to 1 mL with water and was subsequently injected to the Au(III) solution under magnetic stirring (1,500 rpm). The stirring was stopped after 2 min. The seed solution was aged at room temperature for 30 min before use. (3) AuNRs growth: When the growth solution became colorless, a certain volume of HCl (37 wt.% in water, 12.1 M) was added to adjust the pH of the growth solution, after which the solution was kept under stirring for another 15 min. Ascorbic acid (0.064 M) was added into the solution, followed by vigorous agitation for 30 s. Finally, an appropriate volume of seed solution was injected into the growth solution to initiate the AuNRs growth. The mixture was stirred for 30 s and left undisturbed at 30 °C for AuNRs growth. The final products were isolated by centrifugation at 4,000 rpm for 25 min followed by the removal of supernatant. No size and/or shape-selective precipitation was performed. The effect of the addition sequence of bromide and silver was studied, as illustrated in Scheme 1. The concentrations of $HAuCl_4$ and ascorbic acid were kept at 0.5 and 0.154 mM, respectively. More details are presented in the Electronic Supplementary Material (ESM).

2.3 Preparation of CTA-Br-Ag-Br (CTABSB)

In a typical experiment, 12.5 mL of 0.93 M $AgNO_3$ aqueous solution was added drop-wise into 100 mL of 0.27 M aqueous solution of CTAB under vigorous stirring at room temperature. The as-obtained white precipitate was washed with distilled water three times and then dried in vacuum for 2 h.

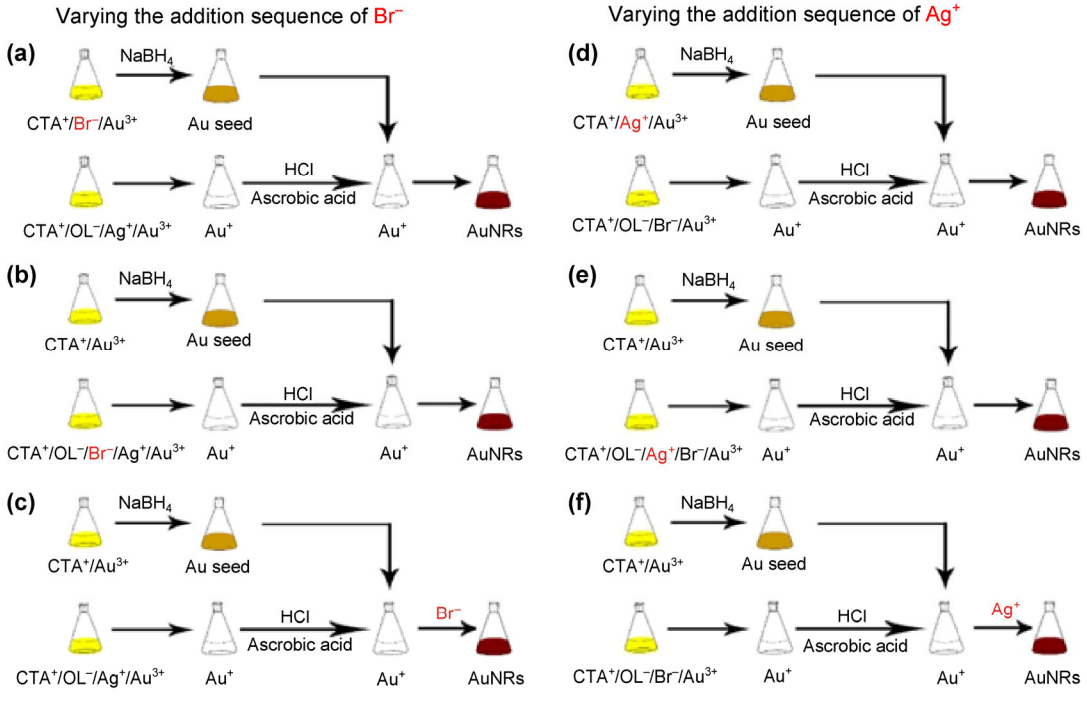

Scheme 1 Schematic illustration of the effect of the addition sequence of (a)–(c) Br^- and (d)–(f) Ag^+. Br^- was added into (a) the seed solution; (b) the growth solution; and (c) after mixing the growth solution and seed solution. And Ag^+ was added into (d) the seed solution; (e) the growth solution; and (f) after mixing the growth solution and seed solution. It is found that high-quality AuNRs can be obtained in all cases.

2.4 Preparation of CTA-Br-Ag-Cl (CTABSC)

In a typical experiment, 1.6 mmoL of CTAC was first dissolved in 50 mL of water, followed by the simultaneous injection of 0.8 mL KBr (0.2 M) and 0.8 mL $AgNO_3$ (0.2 M) of solution under vigorous magnetic agitation (1,500 rpm) for 30 min at room temperature. After that, the mixed solution was dried by rotary evaporation to get the complexes of CTABSC.

2.5 Characterization

Transmission electron microscopy (TEM) characterization was conducted by using a LaB6 TEM (TECNAI G2, FEI), operating at 200 kV. The UV–vis spectra were collected by using the LAMBDA 750 spectrograph (PERKINELMER, USA) in the spectral range of 300–1,200 nm. Scanning electron microscopy (SEM) images were taken at 5 kV by using the Supra 55 SEM from Carl Zeiss, Germany. Mass spectroscopy was carried out with a MALDI-TOF-MS from Micromass, UK in the range of *m*/*z* 60–800 without using a matrix. X-ray diffraction (XRD) patterns were collected by using a Shimadzu XRD-6000 X-ray diffractometer equipped with Cu Kα radiation (λ = 0.15406 nm). Nuclear magnetic resonance (NMR) spectroscopy was obtained on a Varian Unity INOVA 400NB with deuterated chloroform ($CDCl_3$) as the solvent.

3 Results and discussion

To study systematically the effects of Br^- in the seeded growth process, CTAC and NaOL were used as the surfactants and KBr was used as the Br^- source. As illustrated in Scheme 1, KBr was introduced into the system at three different stages: (a) formation of seeds; (b) and (c) growth of seeds: (b) before or (c) after the injection of seeds. The concentration of Br^- in all three cases was kept at 0.16 mM, which is much lower than the concentrations used in most other reports (100 mM). In the first case (Scheme 1(a)), when KBr was added for the formation of seeds, the outcome appears to be the same as that of the seeds prepared by using CTAB. The seed solution exhibited a light brownish color and size of the seed particles was around 3–4 nm. High-resolution TEM (HRTEM) images showed that the lattice distances of Au seeds obtained by using either CTAB or CTAC/KBr as the capping ligand can be indexed as Au (111) (Fig. S1 in the ESM). A representative TEM image of AuNRs obtained is shown in Fig. 1(a), which suggests that the combination of CTAC and KBr works well for AuNRs growth. It is well known that the seed structure is critical to the morphology of the final product, while the seed structure is determined by several factors, including capping ligand, reductant, and reaction temperature [49]. To the best of our knowledge, there is no report on the synthesis of AuNRs from CTAC-capped seeds yet.

In the second approach (Scheme 1(b)), where CTAC was used as the sole capping ligand during seed formation, no obvious difference between the resultant $CTAB^-$ and CTAC-capped seeds was observed. HRTEM image of Au seeds obtained by using CTAC as the capping ligand shows that the size of the Au seed is around 4–5 nm, and the lattice distance can also be indexed as Au (111) (Fig. S2(c) in the ESM). High-quality AuNRs were obtained when KBr (0.16 mM in the final solution) was added to the growth solution (Fig. 1(b)). This result confirmed that CTAC-capped seed could be used to generate high-quality AuNRs.

In the third scenario (illustrated in Scheme 1(c)), the injection of Br^--free seed solution did not initiate the reduction process if no Br^- was present, as indicated by the fact that the growth solution remains colorless and stable for several days. When KBr solution was introduced, the colorless solution gradually became light reddish, bluish, and eventually brownish, confirming the formation of monodispersed AuNRs (Figs. 1(c) and 1(d)).

Therefore, it appears that high-quality AuNRs can be synthesized no matter when Br^- was introduced into the reaction mixture. Our results confirm that Br^- is an essential ingredient for the formation of AuNRs. The aspect ratio of AuNRs can be readily adjusted by controlling the reaction conditions presented for all three approaches. Taking the third one (Scheme 1(c)) as an example, where Br^- was injected after mixing the growth solution and Br^--free seed solution, it was found that the SPR wavelengths could be continuously tuned from 620 to 1,020 nm (Figs. 1(e) and 1(f))).

Compared to Br^-, much less research effort has been devoted to understanding the consequence of

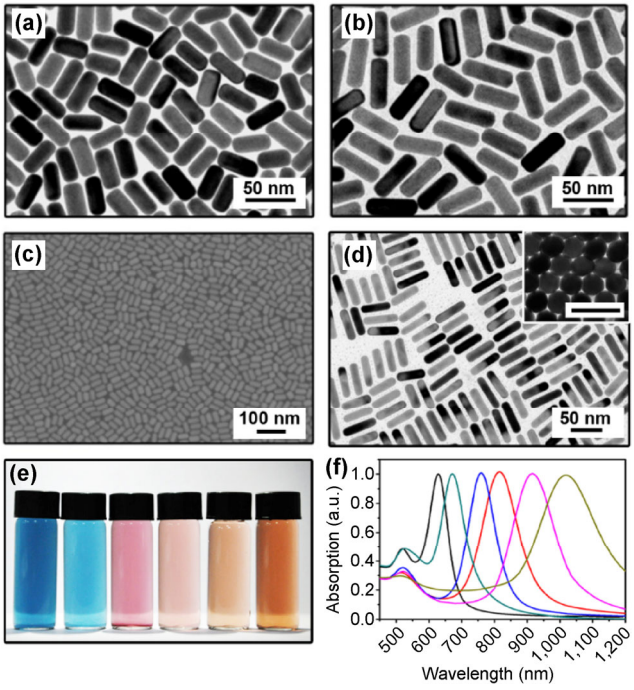

Figure 1 TEM (a), (b), and (d) and SEM image (c) of AuNRs obtained when KBr solution was added into (a) the seed solution; (b) the growth solution; and (c) and (d) after mixing the growth solution and seed solution. The inset in (d) shows the TEM image of vertically standing domains of AuNRs. The scale bar in the inset is 50 nm. Photograph (e) and UV–vis spectra (f) of AuNRs obtained by varying the reaction conditions, when Br^- was added after mixing the seed solution and growth solution. The average dimensions (length, diameter) of the AuNRs (a)–(c) are (47.3 nm, 16.5 nm), (50.2 nm, 17.1 nm), and (52.7 nm, 17.4 nm), respectively.

Ag^+ introduced into the reaction mixture. Here we also investigated the effects of Ag^+ by altering the addition sequence, as illustrated in Schemes 1(d)–1(f). In the first case (Scheme 1(d)), Au nanoparticles with size around 3–5 nm could be obtained when Ag^+ was added into the seed solution (Fig. S2(d) in the ESM). The resultant AuNRs were very uniform (Fig. S3(a) in the ESM). In contrast, the reaction mixture remained colorless in the absence of Ag^+ for several hours, and only spherical Au nanoparticles were obtained after 24 h (Scheme 1(f)). When Ag^+ was added after mixing the seed solution and growth solution, the color of the mixture quickly changed from colorless to brownish within around 15 min and high-quality AuNRs were obtained (Fig. S3(d) in the ESM). It is worth pointing out that Ag^+ should be added before the formation of Au spherical nanoparticles, as evidenced by the fact that low yields of AuNRs (morphological yield <10%) were observed when Ag+ was injected after the reaction mixture became reddish. These observations suggest that Ag^+ ions are critical during the early stage of AuNRs formation.

When CTAB was replaced by a mixture of CTAC and KBr, one notable feature is the dramatically reduced reaction time. Most reported protocols using CTAB-capped seeds and CTAB growth solution usually take several hours to ensure the synthesis of high-quality AuNRs. Although there are several reports on the fast synthesis of AuNRs, they usually suffer from some draw-backs, including low morphological yield and narrow tunability. When CTAC-capped instead of CTAB-capped seeds were employed while still using CTAB in the growth solution, the reaction system required about 7 h to complete (black curve in Fig. 2(a)). On the other hand, the reaction could be completed within 45 min when CTAB-capped seeds and CATC growth solution were used (red curve in Fig. 2(a)). The reaction can be further accelerated by replacing CTAB in the growth solution with a combination of CTAC and Br^-. Remarkably, all three variations were found to reach a plateau within about 15 min ([Br^-] = 0.16 mM). When the concentration of Br^- is increased, an obvious S-shaped plot can be observed, indicating a possible incubation time before the formation of AuNRs. This phenomenon can be attributed to the stronger complex ability of bromide and Au. As a result, the reduction reaction is retarded.

Furthermore, these results indicate that a high concentration of Br^- can slow down the growth of AuNRs, which is in agreement with the observation by Raston and co-workers [50]. To better understand why bromide ions can retard the growth of AuNRs, matrix-assisted laser desorption/ionization time-of-flight mass spectrometry was used to analyze the complexes formed between gold and Br^- ions. As shown in Fig. S4 in the ESM, a sharp peak at the m/z of 357.07, attributed to $AuBr_2^-$, was observed in the CTAB growth solution. As a result, the slower reaction rate can be explained by the formation of $AuBr_2^-$ in the presence of higher concentration of Br^-.

It is clear that high-quality AuNRs can be obtained as long as CTA^+, Br^-, and Ag^+ ions were simultaneously present before the reduction of gold precursor commences. A series of experiments were conducted

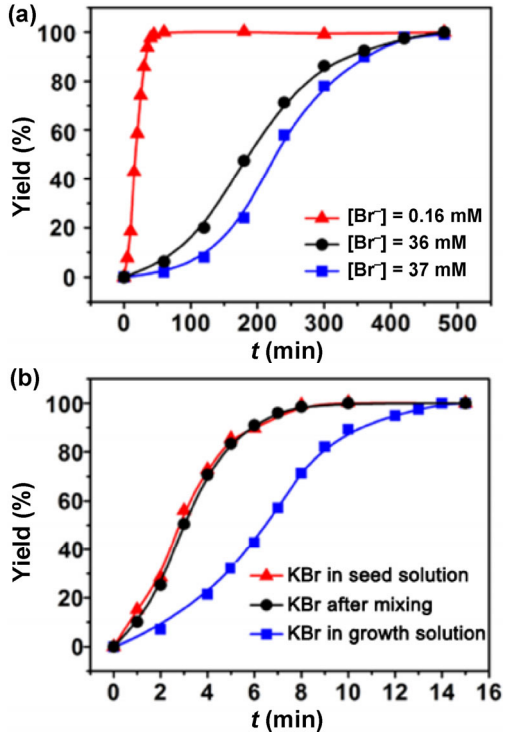

Figure 2 Plots of the reaction progress as a function of reaction time. (a) AuNRs were obtained by using: (red triangle) CTAB capped seed and CTAC growth solution; (black dot) CTAC capped seed and CTAB growth solution; (blue square) CTAB capped seed and CTAB growth solution. (b) AuNRs were obtained when CTAC was used as the sole surfactant and KBr was added into (red triangle) seed solution; (black dot) after mixing the growth solution and seed solution; and (blue square) growth solution. The concentration of Br^- is 0.16 mM in all three cases (b). Detailed reaction conditions are listed in Table S1 (in the ESM).

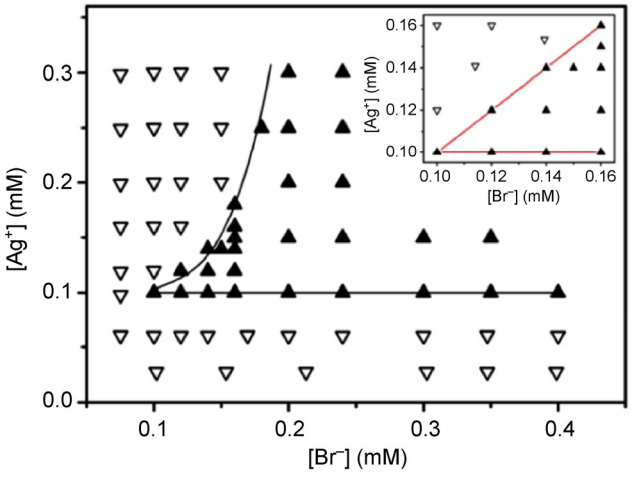

Figure 3 Scatter plots showing the correlation between the concentration of bromide and silver ions during AuNR formation. The solid triangles correspond to successful preparation of AuNRs (defined as a product yield higher than 90%), while the hollow ones indicate dramatically lower yield (lower than 50%). The inset shows the linear correlation between Br^- and Ag^+ when both are approaching the low-limiting concentrations (0.1 mM for both).

to figure out the correlation among these three components. As shown in Fig. 3, there exists a lower limit for the concentrations of both silver and bromide ions. AuNRs with a morphological yield higher than 90% can be synthesized when both the concentrations of silver ions and bromide ions exceed 0.1 mM. Importantly, when both species approach the threshold concentrations of 0.1 mM, a linear correlation between them was observed, which is highlighted in the inset of Fig. 3. The concentration of Br^- should be equal or higher than that of Ag^+. This is the first time that such a correlation between Ag^+ and Br^- is uncovered. The concentration of Br^- used in existing protocols was generally much higher than that of Ag^+. As a result, many research groups have conjectured that the complex of CTA-Br-Ag-Br could play an important role in determining the formation of anisotropic AuNRs.

For instance, Hubert et al. successfully prepared AuNRs by using the CTA-Br-Ag-Br complex [46]. Recent density functional theory (DFT) calculations by Almora-Barrios and co-workers demonstrated that this complex could preferentially adsorb onto certain facets of the seeds, blocking them from growth, and promoting the formation of anisotropic AuNRs [51].

In contrast, our results indicate that the primary complex responsible for AuNR growth is CTA-Br-Ag^+, in the form of either CTABSB or CTABSC. With a fixed Br^-/Ag^+ ratio of 1, monodisperse AuNRs with tunable dimensions and SPR properties can be prepared by simply varying the concentrations of Ag^+ and Br^- (Fig. S5 in the ESM). It is worth pointing out that when the concentrations of Br^- and Ag^+ are higher than 0.2 mM, monodisperse AuNRs could be obtained even when the concentration of Ag^+ is higher than Br^-. It is believed that there is a minimum required concentration of both Br^- and Ag^+. The formation rate of AuNRs is influenced by the concentration of both Br^- and Ag^+. When the concentrations of Br^- and Ag^+ are increased accordingly, the reaction rate decreased gradually, as evidenced by the slower color change.

The minimal required concentration of CTA^+ was also studied. Jin and co-workers found that AuNRs

could be obtained even when the CTAB concentration was as low as 0.5 mM, which is lower than the critical micelle concentration (cmc) of CTAB (~1 mM at room temperature) [41]. However, in that case, the concentration of Br^- was still at 0.1 M and the morphological yield of AuNRs was marginal. We carried out a set of experiments in which both the concentrations of Ag^+ and Br^- were fixed at 0.16 mM. When the concentration of CTAC was 0.5 mM, only large spherical nanoparticles were obtained. Gold nanoparticles with an aspect ratio of about 1.43 could be prepared when CTAC concentration was only 0.9 mM (Figs. S6 and S7 in the ESM), which is still lower than the cmc of CTAC (1.3 mM at 30 °C) [52]. Increasing the CTAC concentration to 3.7 mM led to the formation of elongated nanoparticles, which points to the shape-promoting effects of CTA^+. Further increasing CTAC concentration to 9.8 mM resulted in the formation of AuNRs. The length of AuNRs remained almost constant while the diameter decreased dramatically when the concentration of CTAC was increased.

Based on these experimental observations, we propose that the most important factor in determining AuNR growth is the formation of $[CTA\text{-}Br\text{-}Ag]^+$ complex ions. The counter ion can be either bromide (forming CTA-Br-Ag-Br), or chloride (forming CTA-Br-Ag-Cl). To further confirm the proposed mechanism, two complexes, namely CTABSB [52] and CTABSC, were synthesized. The XRD pattern of the CTABSB complex is shown in Fig. 4(a). It is believed that the $C_{19}H_{42}NAgBr_2$ compound has a layered structure with the AgBr monolayer bound to interdigitated CTAB

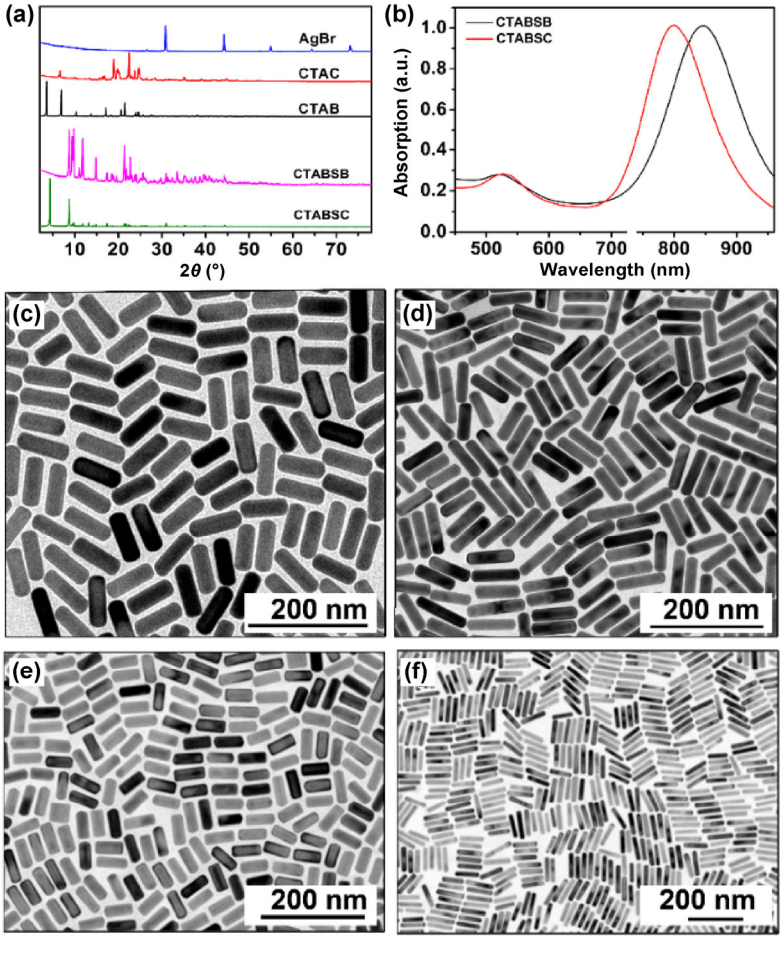

Figure 4 (a) Powder XRD patterns of different compounds: (from top to bottom) AgBr, CTAC, CTAB, CTA-Br-Ag-Br, and CTA-Br-Ag-Cl; (b) UV–vis spectra of AuNRs prepared by using CTA-Br-Ag-Cl (black curve) and CTA-Br-Ag-Br (red curve) as the ligands; (c) and (d) TEM images of AuNRs prepared by using (c) CTA-Br-Ag-Cl and (d) CTA-Br-Ag-Br as the ligand. TEM images of AuNRs prepared by dissolving AgBr crystals in (e) CTAC and (f) CTAB solution.

layers [53, 54]. It is worth mentioning that our efforts in synthesizing CTACSC turned out to be unsuccessful, and only AgCl precipitates were obtained when CTA^+, Ag^+ and Cl^- were mixed (Fig. S8 in the ESM). The as-prepared complexes are very stable. After being stored under ambient condition for three months, no obvious change was observed from XRD measurements. XPS measurements show that the ratios between Br and Ag are about 2.12/1.00 in CTA-Br-Ag-Br and 1.13/1.00 in CTA-Br-Ag-Cl (Figs. S10 and S11). Both CTABSB and CTABSC complexes were used as ligands to prepare high-quality AuNRs (Figs. 4(b)–4(d)).

Although AgBr is an insoluble compound in pure water (K_{sp} = 5.4 × 10^{-13}), small amounts of AgBr are soluble in a CTAB micelle solution. It is found that AgBr can also be used to synthesize AuNRs. Certain amount of AgBr (the final concentration of Ag^+ in the growth solution was fixed at 0.16 mM) was dissolved in CTAC or CTAB solution by ultrasonication. Figure 4(e) shows the TEM image of AuNRs prepared by dissolving AgBr into the CTAC growth solution. The average length is ~52.4 nm and the diameter is about 21.3 nm, giving rise to a LSPR peak at ~800 nm (Fig. S12 in the ESM). Monodisperse AuNRs could also be prepared by dissolving AgBr powders into a CTAB growth solution (Fig. 4(f)). Other similar complexes including DTA-Br-Ag-Cl, TTA-Br-Ag-Cl, and OTA-Br-Ag-Cl with different alkyl chain lengths were also effective in promoting the formation of AuNRs (Fig. S14 in the ESM).

4 Conclusions

In conclusion, we have demonstrated that the most critical factor in the seeded growth of AuNRs is the complex, CTA-Br-Ag^+, which can selectively bind onto certain facets of Au seeds and facilitate the formation of anisotropic nanostructures. On the basis of this improved understanding of the mechanism, we have refined the synthesis by replacing CTAB with a mixture of CTAC and KBr. More effort is currently being devoted to growing large single crystals of CTA-Br-Ag-Br and CTA-Br-Ag-Cl and analyzing their crystal structures. Remarkably, monodisperse AuNRs can be obtained within 15 min after seed injection, which is much faster than existing protocols that take several hours. We have also shown that AgBr, which forms the CTA-Br-Ag^+ complex upon adding to the CTAB or CTAC solution, can be used directly for AuNR synthesis. This work represents an important step toward a better understanding of the mechanism of AuNRs synthesis.

Acknowledgements

We acknowledge the Collaborative Innovation Center of Suzhou Nano Science & Technology, the SWC Center for Synchrotron Radiation Research, the Priority Academic Program Development of Jiangsu Higher Education Institu-tions, the National Natural Science Foundation of China (Nos. 21401135 and 21673150) and the Natural Science Foundation of Jiangsu Province (No. BK20140304) for funding support.

Electronic Supplementary Material: Supplementary material (experimental details, digital images of seed solution, matrix-assisted laser desorption ionization-time of flight-mass spectrometry spectra (MALDI-TOF-MS), ^{1}H-NMR spectra, additional UV–vis spectra, TEM images and XPS data) is available in the online version of this article at http://dx.doi.org/10.1007/s12274-016-1404-3.

References

[1] Huang, X.; Zeng, Z. Y.; Bao, S. Y.; Wang, M. F.; Qi, X. Y.; Fan, Z. X.; Zhang, H. Solution-phase epitaxial growth of noble metal nanostructures on dispersible single-layer molybdenum disulfide nanosheets. *Nat. Commun.* **2013**, *4*, 1444.

[2] Peng, S.; Lei, C. H.; Ren, Y.; Cook, R. E.; Sun, Y. G. Plasmonic/magnetic bifunctional nanoparticles. *Angew. Chem., Int. Ed.* **2011**, *50*, 3158–3163.

[3] Fu, C. H.; He, C. F.; Tan, L. F.; Wang, S. H.; Shang, L.; Li, L. L.; Meng, X. W.; Liu, H. Y. High-yield preparation of robust gold nanoshells on silica nanorattles with good biocompatiblity. *Sci. Bull.* **2016**, *61*, 282–291.

[4] Mettela, G.; Kulkarni, G. U. Facet selective etching of Au microcrystallites. *Nano Res.* **2015**, *8*, 2925–2934.

[5] Ma, L. G.; Huang, Z. H.; Duan, Y. Y.; Shen, X. F.; Che, S. Optically active chiral Ag nanowires. *Sci. China Mater.* **2015**, *58*, 441–446.

[6] Chen, H. J.; Shao, L.; Li, Q.; Wang, J. F. Gold nanorods and their plasmonic properties. *Chem. Soc. Rev.* **2013**, *42*, 2679–2724.

[7] Wijaya, A.; Schaffer, S. B.; Pallares, I. G.; Hamad-Schifferli, K. Selective release of multiple DNA oligonucleotides from gold nanorods. *ACS Nano* **2009**, *3*, 80–86.

[8] Grabinski, C.; Schaeublin, N.; Wijaya, A.; D'Couto, H.; Baxamusa, S. H.; Hamad-Schifferli, K.; Hussain, S. M. Effect of gold nanorod surface chemistry on cellular response. *ACS Nano* **2011**, *5*, 2870–2879.

[9] Liu, N.; Tang, M. L.; Hentschel, M.; Giessen, H.; Alivisatos, A. P. Nanoantenna-enhanced gas sensing in a single tailored nanofocus. *Nat. Mater.* **2011**, *10*, 631–636.

[10] Wang, L. B.; Zhu, Y. Y.; Xu, L. G.; Chen, W.; Kuang, H.; Liu, L. Q.; Agarwal, A.; Xu, C. L.; Kotov, N. A. Side-by-side and end-to-end gold nanorod assemblies for environmental toxin sensing. *Angew. Chem., Int. Ed.* **2010**, *49*, 5472–5475.

[11] Huh, Y. M.; Jun, Y. W.; Song, H. T.; Kim, S.; Choi, J. S.; Lee, J. H.; Yoon, S.; Kim, K. S.; Shin, J. S.; Suh, J. S. et al. *In vivo* magnetic resonance detection of cancer by using multifunctional magnetic nanocrystals. *J. Am. Chem. Soc.* **2005**, *127*, 12387–12391.

[12] Rosi, N. L.; Mirkin, C. A. Nanostructures in biodiagnostics. *Chem. Rev.* **2005**, *105*, 1547–1562.

[13] Huschka, R.; Zuloaga, J.; Knight, M. W.; Brown, L. V.; Nordlander, P.; Halas, N. J. Light-induced release of DNA from gold nanoparticles: Nanoshells and nanorods. *J. Am. Chem. Soc.* **2011**, *133*, 12247–12255.

[14] Huang, X. H.; Neretina, S.; El-Sayed, M. A. Gold nanorods: From synthesis and properties to biological and biomedical applications. *Adv. Mater.* **2009**, *21*, 4880–4910.

[15] Dreaden, E. C.; Alkilany, A. M.; Huang, X. H.; Murphy, C. J.; El-Sayed, M. A. The golden age: Gold nanoparticles for biomedicine. *Chem. Soc. Rev.* **2012**, *41*, 2740–2779.

[16] Hirsch, L. R.; Stafford, R. J.; Bankson, J. A.; Sershen, S. R.; Rivera, B.; Price, R. E.; Hazle, J. D.; Halas, N. J.; West, J. L. Nanoshell-mediated near-infrared thermal therapy of tumors under magnetic resonance guidance. *Proc. Natl. Acad. Sci. USA* **2003**, *100*, 13549–13554.

[17] Durr, N. J.; Larson, T.; Smith, D. K.; Korgel, B. A.; Sokolov, K.; Ben-Yakar, A. Two-photon luminescence imaging of cancer cells using molecularly targeted gold nanorods. *Nano Lett.* **2007**, *7*, 941–945.

[18] Huang, X. H.; El-Sayed, I. H.; Qian, W.; El-Sayed, M. A. Cancer cells assemble and align gold nanorods conjugated to antibodies to produce highly enhanced, sharp, and polarized surface Raman spectra: A potential cancer diagnostic marker. *Nano Lett.* **2007**, *7*, 1591–1597.

[19] Liu, Y. L.; Yang, M.; Zhang, J. P.; Zhi, X.; Li, C.; Zhang, C. L.; Pan, F.; Wang, K.; Yang, Y. M.; de la Fuentea, J. M. et al. Human induced pluripotent stem cells for tumor targeted delivery of gold nanorods and enhanced photothermal therapy. *ACS Nano* **2016**, *10*, 2375–2385.

[20] Rycenga, M.; McLellan, J. M.; Xia, Y. N. Controlling the assembly of silver nanocubes through selective functionalization of their faces. *Adv. Mater.* **2008**, *20*, 2416–2420.

[21] Tao, A.; Kim, F.; Hess, C.; Goldberger, J.; He, R. R.; Sun, Y. G.; Xia, Y. N.; Yang, P. D. Langmuir-blodgett silver nanowire monolayers for molecular sensing using surface-enhanced Raman spectroscopy. *Nano Lett.* **2003**, *3*, 1229–1233.

[22] Lal, S.; Grady, N. K.; Kundu, J.; Levin, C. S.; Lassiter, J. B.; Halas, N. J. Tailoring plasmonic substrates for surface enhanced spectroscopies. *Chem. Soc. Rev.* **2008**, *37*, 898–911.

[23] Alvarez-Puebla, R. A.; Agarwal, A.; Manna, P.; Khanal, B. P.; Aldeanueva-Potel, P.; Carbó-Argibay, E.; Pazos-Pérez, N.; Vigderman, L.; Zubarev, E. R.; Kotov, N. A. et al. Gold nanorods 3D-supercrystals as surface Enhanced Raman scattering spectroscopy substrates for the rapid detection of scrambled prions. *Proc. Natl. Acad. Sci. USA* **2011**, *108*, 8157–8161.

[24] Xu, Y.; Zhao, Y.; Chen, L.; Wang, X. C.; Sun, J. X.; Wu, H. H.; Bao, F.; Fan, J.; Zhang, Q. Large-scale, low-cost synthesis of monodispersed gold nanorods using a gemini surfactant. *Nanoscale* **2015**, *7*, 6790–6797.

[25] Yu, Y. Y.; Chang, S. S.; Lee, C. L.; Wang, C. R. C. Gold nanorods: Electrochemical synthesis and optical properties. *J. Phys. Chem. B* **1997**, *101*, 6661–6664.

[26] Jana, N. R.; Gearheart, L.; Murphy, C. J. Seed-mediated growth approach for shape-controlled synthesis of spheroidal and rod-like gold nanoparticles using a surfactant template. *Adv. Mater.* **2001**, *13*, 1389–1393.

[27] Busbee, B. D.; Obare, S. O.; Murphy, C. J. An improved synthesis of high-aspect-ratio gold nanorods. *Adv. Mater.* **2003**, *15*, 414–416.

[28] Nikoobakht, B.; El-Sayed, M. A. Preparation and growth mechanism of gold nanorods (NRs) using seed-mediated growth method. *Chem. Mater.* **2003**, *15*, 1957–1962.

[29] Wu, H. Y.; Chu, H. C.; Kuo, T. J.; Kuo, C. L.; Huang, M. H. Seed-mediated synthesis of high aspect ratio gold nanorods with nitric acid. *Chem. Mater.* **2005**, *17*, 6447–6451.

[30] Zhu, J.; Yong, K. T.; Roy, I.; Hu, R.; Ding, H.; Zhao, L. L.; Swihart, M. T.; He, G. S.; Cui, Y. P.; Prasad, P. N. Additive controlled synthesis of gold nanorods (GNRs) for two-photon luminescence imaging of cancer cells. *Nanotechnology* **2010**, *21*, 285106.

[31] Kim, F.; Sohn, K.; Wu, J. S.; Huang, J. X. Chemical synthesis of gold nanowires in acidic solutions. *J. Am. Chem. Soc.* **2008**, *130*, 14442–14443.

[32] Zweifel, D. A.; Wei, A. Sulfide-arrested growth of gold nanorods. *Chem. Mater.* **2005**, *17*, 4256–4261.

[33] Smith, D. K.; Miller, N. R.; Korgel, B. A. Iodide in CTAB

prevents gold nanorod formation. *Langmuir* **2009**, *25*, 9518–9524.

[34] Smith, D. K.; Korgel, B. A. The importance of the CTAB surfactant on the colloidal seed-mediated synthesis of gold nanorods. *Langmuir* **2008**, *24*, 644–649.

[35] Rayavarapu, R. G.; Ungureanu, C.; Krystek, P.; van Leeuwen, T. G.; Manohar, S. Iodide impurities in hexadecyltrimethylammonium bromide (CTAB) products: Lot–lot variations and influence on gold nanorod synthesis. *Langmuir* **2010**, *26*, 5050–5055.

[36] Sau, T. K.; Murphy, C. J. Role of ions in the colloidal synthesis of gold nanowires. *Philos. Mag.* **2007**, *87*, 2143–2158.

[37] Ye, X. C.; Gao, Y. Z.; Chen, J.; Reifsnyder, D. C.; Zheng, C.; Murray, C. B. Seeded growth of monodisperse gold nanorods using bromide-free surfactant mixtures. *Nano Lett.* **2013**, *13*, 2163–2171.

[38] Ye, X. C.; Zheng, C.; Chen, J.; Gao, Y. Z.; Murray, C. B. Using binary surfactant mixtures to simultaneously improve the dimensional tunability and monodispersity in the seeded growth of gold nanorods. *Nano Lett.* **2013**, *13*, 765–771.

[39] Ye, X. C.; Jin, L. H.; Caglayan, H.; Chen, J.; Xing, G. Z.; Zheng, C.; Doan-Nguyen, V.; Kang, Y. J.; Engheta, N.; Kagan, C. R. et al. Improved size-tunable synthesis of monodisperse gold nanorods through the use of aromatic additives. *ACS Nano* **2012**, *6*, 2804–2817.

[40] Lohse, S. E.; Murphy, C. J. The quest for shape control: A history of gold nanorod synthesis. *Chem. Mater.* **2013**, *25*, 1250–1261.

[41] Garg, N.; Scholl, C.; Mohanty, A.; Jin, R. C. The role of bromide ions in seeding growth of Au nanorods. *Langmuir* **2010**, *26*, 10271–10276.

[42] Liu, M. Z.; Guyot-Sionnest, P. Mechanism of silver (I)-assisted growth of gold nanorods and bipyramids. *J. Phys. Chem. B* **2005**, *109*, 22192–22200.

[43] Personick, M. L.; Langille, M. R.; Zhang, J.; Mirkin, C. A. Shape control of gold nanoparticles by silver underpotential deposition. *Nano Lett.* **2011**, *11*, 3394–3398.

[44] Murphy, C. J.; Sau, T. K.; Gole, A. M.; Orendorff, C. J.; Gao, J. X.; Gou, L. F.; Hunyadi, S. E.; Li, T. Anisotropic metal nanoparticles: Synthesis, assembly, and optical applications. *J. Phys. Chem. B* **2005**, *109*, 13857–13870.

[45] Johnson, C. J.; Dujardin, E.; Davis, S. A.; Murphy, C. J.; Mann, S. Growth and form of gold nanorods prepared by seed-mediated, surfactant-directed synthesis. *J. Mater. Chem.* **2002**, *12*, 1765–1770.

[46] Hubert, F.; Testard, F.; Spalla, O. Cetyltrimethylammonium bromide silver bromide complex as the capping agent of gold nanorods. *Langmuir* **2008**, *24*, 9219–9222.

[47] Pérez-Juste, J.; Liz-Marzán, L.; Carnie, S.; Chan, D. Y. C.; Mulvaney, P. Electric-field-directed growth of gold nanorods in aqueous surfactant solutions. *Adv. Funct. Mater.* **2004**, *14*, 571–579.

[48] Jackson, S. R.; McBride, J. R.; Rosenthal, S. J.; Wright, D. W. Where's the silver? Imaging trace silver coverage on the surface of gold nanorods. *J. Am. Chem. Soc.* **2014**, *136*, 5261–5263.

[49] Xia, Y. N.; Xiong, Y. J.; Lim, B.; Skrabalak, S. E. Shape-controlled synthesis of metal nanocrystals: Simple chemistry meets complex physics? *Angew. Chem., Int. Ed.* **2009**, *48*, 60–103.

[50] Bullen, C.; Zijlstra, P.; Bakker, E.; Gu, M.; Raston, C. Chemical kinetics of gold nanorod growth in aqueous CTAB solutions. *Cryst. Growth Des.* **2011**, *11*, 3375–3380.

[51] Almora-Barrios, N.; Novell-Leruth, G.; Whiting, P.; Liz-Marzán, L. M.; López, N. Theoretical description of the role of halides, silver, and surfactants on the structure of gold nanorods. *Nano Lett.* **2014**, *14*, 871–875.

[52] Ito, K.; Ariyoshi, Y.; Tanabiki, F.; Sunahara, H. Anion chromatography using octadecylsilane reversed-phase columns coated with cetyltrimethylammonium and its application to nitrite and nitrate in seawater. *Anal. Chem.* **1991**, *63*, 273–276.

[53] Liu, X. H.; Luo, X. H.; Lu, S. X.; Zhang, J. C.; Cao, W. L. A novel cetyltrimethyl ammonium silver bromide complex and silver bromide nanoparticles obtained by the surfactant counterion. *J. Colloid Interface Sci.* **2007**, *307*, 94–100.

[54] Calabrese, J.; Jones, N. L.; Harlow, R. L.; Herron, N.; Thorn, D. L.; Wang, Y. Preparation and characterization of layered lead halide compounds. *J. Am. Chem. Soc.* **1991**, *113*, 2328–2330.